

Micro-Modeling for Enhanced Porosity-Permeability Relationships

Jeff Boisvert, John Manchuk, Chad Neufeld, Eric Niven and Clayton V. Deutsch

Accurate modeling of vertical and horizontal permeability in oil sands is difficult due to the lack of representative permeability data. Core plug data could be used to model permeability through the inference of a porosity-permeability relationship. The drawbacks of this approach include (1) variability and uncertainty in the porosity-permeability scatter plot as a result of sparse sampling and (2) biased core plug data taken preferentially from sandy or homogeneous intervals. A two-step process can be used where core photographs and core plug data are used to assess small scale permeability followed by upscaling to a representative geomodeling cell size. This paper expands on a methodology that utilizes core photographs to infer porosity-permeability relationships. This methodology is robust because there is abundant core photograph data available compared to core plug permeability samples and the bias due to preferential sampling can be avoided. The proposed methodology entails building micro-scale models with 0.5 mm cells conditional to 5cm x 5cm sample images extracted from core photographs. The micro-models are sand/shale indicator models with realistic permeability values ($k_{sand} \approx 7000\text{mD}$, $k_{shale} \approx 0.5\text{mD}$). The spatial structure of the micro-model controls the resulting porosity-permeability relationships that are obtained from upscaling. Previously, these models were generated with sequential indicator simulation (SIS). However, SIS may not capture the spatial structure of the complex facies architecture observed in core photographs. Models based on multiple point statistics and object based techniques are proposed to enhance realism. Micro-models are upscaled to the scale of the log data (5 cm in this case) with a steady-state flow simulation to determine the porosity-permeability relationship. The porosity-permeability relationships for geomodeling, or flow simulation, can be determined with subsequent mini-modeling and further upscaling. The resulting porosity-permeability relationship can be used to populate reservoir models and enhance traditional core data. Wells from the Nexen Inc. Long Lake Phase 1 site in the Alberta Athabasca oil sands region are used to demonstrate the methodology.

Introduction

The Alberta oil sands are a vast resource with proven reserves of 169.9 billion barrels (Government of Alberta, 2011). Although surface mining techniques have been used in the oil sands since the late 1960's and are still used today, the majority of reserves are too deep for mining to be economical. As a result, in-situ recovery methods are required. Since bitumen is more viscous than conventional oil, steam is often injected to raise the temperature of the bitumen, reducing its viscosity and allowing it to be pumped to surface. The most widely used in-situ recovery method in the oil sands is steam-assisted gravity drainage (SAGD). Engineers use flow simulation to make predictions of steam rise and oil and water drainage. A critical input parameter in the flow simulation of SAGD operations is vertical permeability.

There are two main reservoir facies associations of concern in the McMurray. The first is the massive cross-stratified coarse sands with high porosity, permeability and oil saturation. This is the most desirable reservoir facies. The second facies association is inclined heterolithic stratification (IHS). These heterogeneous deposits form as a result of lateral growth of point bars within meandering channels of freshwater rivers and creeks draining inter-tidal mudflats. IHS deposits are generally decimeter to meter-thick repetitive sets of inclined beds of sand and mud and can range in quality from mostly sandy to mostly muddy (Thomas et al., 1987). A third facies association, Breccia, is also found in small amounts near the base of a channel succession due to the erosion and collapse of previous muddy point bars.

The geology of the McMurray formation has a large influence on its vertical permeability profile. Permeability is controlled by grain size, sorting and sediment type (Olson, Yaich and Holder, 2009; Shang and Wang, 2011). Vertical permeability is typically inversely related to the horizontal continuity of the sediments. For example, where horizontal continuity is low, there are flow paths around low permeability units. Where horizontal continuity is high, vertical permeability is decreased because there are few flow paths around the low-permeability units.

A number of issues make estimating permeability difficult. The scale of core plugs compared to the scale of geomodeling or flow simulation must be accounted for (Tran, 1996) as the vertical permeability at the whole core scale is what would be most important for SAGD. Preferential sampling of core is another issue. Core plug samples are often taken preferentially from the clean sand; otherwise, samples would have a high tendency to break or deteriorate prior to lab testing. This preferential sampling results in bias and an incomplete permeability to porosity relationship that is difficult to infer. Permeability inference is further confounded because core plug porosity and permeability data cannot be calibrated with well-test data because bitumen is immobile under in-situ temperature and pressure conditions. There are a number of common approaches to estimate permeability in oil sands:

1. A constant horizontal and vertical permeability could be assigned within each facies. If the permeability variation within a single facies is small compared to the permeability variation between facies, this simplification could be acceptable.

2. Regression models of the log of permeability versus porosity can be constructed for each facies. Then the log derived porosity data can be transformed to permeability within each facies. The main limitation of regression approaches is that they do not account for the uncertainty in permeability for a given porosity.

3. A cloud transformation (Kolbjornsen and Abrahamson, 2004) technique could be used to attempt to account for the statistical variation in permeability.

4. A p-field simulation technique (Deutsch, 2002) could be used where the values from a correlated random field are used in the Monte-Carlo simulation to draw permeability values. The realizations of permeability will then have the correct spatial variation.

Although the aforementioned techniques are valid and useful, the overall estimation of vertical permeability can be improved by considering all available information. Core photographs or full-bore formation micro-images (FMIs) are one source of fine scale information. Facies and permeability can be assigned to the core photograph on a pixel-by-pixel basis. Individual pixels can be classified as either sand or shale. There is no mixing of facies to consider at this resolution. The micro-scale model can be upscaled to an effective porosity and permeability at the scale corresponding to the image size. The advantage of this methodology is that it considers all available data, permitting improved predictions of vertical permeability, while resolving the aforementioned scaling and non-representative sampling issues.

This paper presents a methodology to use the 2D core photographs to calculate 3D geostatistical models of porosity and permeability for each facies at the scale of the image pixels. The micro-models are upscaled using flow simulation to calculate an effective vertical and horizontal permeability at a 5 cm scale. The methodology is applied to wells located in the Nexen, Inc. Long Lake Phase 1 Site.

Methodology

The goal of this work is to determine upscaled porosity (ϕ)-horizontal permeability (k_h) and k_h -vertical permeability (k_v) relationships that can be used in a cloud transformation for inference of reservoir properties for flow simulation. The upscaled ϕ - k_h and k_h - k_v relationships for a particular facies are inferred by analyzing core photographs. The main idea is to generate a 3D model of permeability at a scale where the model cell size is such that each cell can be assumed entirely sand or entirely shale which simplifies permeability assignment. In this work, the models are built at the approximate resolution of the core photographs (0.5mm x 0.5mm x 0.5mm blocks). This resolution is used to capture the small scale variations in sand/shale; clearly, the size of the sand grains would make the actual flow properties of such a small volume difficult to infer.

The core photograph provides the necessary data for assignment of sand and shale in a 3D indicator micro-model. A distribution of permeability is assumed within the sand and shale categories. Flow simulation is used to determine an upscaled porosity-permeability relationship for the sand/shale mixture. Deutsch (2010) provides a detailed methodology for generating upscaled porosity-permeability relationships from core photographs or FMI data and the methodology is summarized in this section. This work considers core photographs but these techniques could be extended to consider FMI data. The methodology:

1. Digitize the core photograph and select a cutoff value

2. Infer a 3D model of permeability with SIS followed by SGS
3. Flow simulation to determine the upscaled permeability
4. Repeat for multiple core photographs

The main driver of flow is the sand/shale spatial arrangement. The goal of this work is to improve upon the generation of the sand/shale indicator models to better capture the flow behavior of different facies. In past work, a variogram was automatically inferred from the 2D core photograph and SIS was used to generate a 3D indicator model. The appropriateness of using SIS to generate the indicator models depends on the facies considered; the focus here is specific to the McMurray Formation and the facies present can be broadly classified as sand, IHS and breccia. Techniques specific to each facies type are explored.

Details of the standard micro-modeling methodology are expanded upon below.

Step 1: Digitize the core photograph

The locations of the extracted models are manually selected from the core photographs (Figure 1). A representative range of core photograph samples should be selected such that the range of porosity values in the log data are represented in the micro-models. This is accomplished by selecting models with various proportions of shale. The images are 5cm by 5cm with 100 cells in each direction. It is more convenient to work in pixels and models are shown to be 100 x 100 with 0.5mm blocks throughout. Gray scale cutoff values are selected to assign sand and shale categories. The appropriate cutoff value for a model varies for each photograph because of local lighting conditions, water saturations, etc. For each model this cutoff value is selected by examining a range of cutoffs and determining the most visually appropriate value (Figure 1). The cutoff value is a key parameter as it controls the spatial distribution of categories.

Step 2: Infer the 3D permeability model

The result of Step 1 is a 2D indicator model of sand and shale. While this model could be used in a 2D flow simulation, the three dimensional characteristics of flow would not be captured. SIS is typically used to generate the 3D categorical model and requires a variogram model. The conditioning data, in the form of a 2D model of sand/shale, provides the necessary data for inference of the vertical and horizontal variograms (Figure 2). The continuity in the second horizontal direction (into the page in Figure 1) is assumed to be the same as the horizontal direction in the core photograph. The validity of this assumption is the focus of the first part of this work and is discussed further below.

SIS is implemented with the variogram model and the conditioning data provided by the core photograph (Figure 3). Ten realizations of sand/shale are generated to assess the uncertainty in the upscaled results. The number of realizations could be increased; however, multiple core photographs are considered for each facies and the large number of flow simulations quickly becomes CPU demanding.

Flow simulation requires a model of permeability. SGS is used to populate the categorical models with realistic permeability values. Due to the small scale of the individual cells in this model and the assumption that each cell is either entirely sand or entirely shale, a k_v/k_h ratio of ~ 1.0 is reasonable. The permeability distribution for sand is assumed to approximately match the core samples taken in sand $N(7000 \text{ mD}, 2500 \text{ mD})$. There are no core samples taken in shale; a realistic distribution of $N(0.5 \text{ mD}, 0.1 \text{ mD})$ is assumed. Adjusting these distributions has an effect on the upscaled porosity-permeability relationships and is roughly calibrated to existing core samples and previous experience with similar deposits.

Step 3: Flow simulation to determine upscaled permeability

A steady state flow simulation using FLOWSIM provides the upscaled k_v and k_h values for each 3D micro-model; however, there is no porosity value for each model and it must be inferred. It would be inappropriate to use log porosity data as the volume of influence is much larger than the 5cm x 5cm models considered. The porosity for shale is assumed to be 1% and sand is assumed to be 40%; the proportion weighted average (Equation 1) provides the porosity for each realization. Equation 1 is a good approximation for porosity but assumes perfectly clean sand without interstitial clays and could be

modified given site specific considerations. Equation 1 is a good approximation for porosity but assumes perfectly clean sand without interstitial clays and could be modified given site specific considerations.

$$\phi_{\text{realization}} = 0.4 (\rho_{\text{sand}}) + 0.01 (\rho_{\text{shale}}) \quad (1)$$

Case Study

The methodology as presented above relies on SIS for the generation of the sand/shale categories within each facies modeled. In this section, modeling considerations specific to the sand/shale geometry of each facies are incorporated into micro-modeling. Core photographs, core samples and log data from 12 wells in the Long Lake Phase 1 project in the Athabasca oil sands region of Alberta, Canada are used to demonstrate the methodology. There are three identified facies of interest: sand, IHS and breccia (Figure 4). Based on log data, the proportions of facies in the reservoir are 60% sand, 29% IHS and 11% Breccia.

The core data is not used explicitly for calibration nor in selecting micro-model locations as it is not typically representative of in-situ reservoir properties (i.e. porosity) due to the difficulty of sampling high shale proportions. This issue is highlighted in Table 1 where the average porosity (and even permeability) of IHS and Breccia are similar to the samples in sand. Core data alone cannot provide sufficient information to fully infer the relationship between porosity and permeability.

Table 1: Available data.

Facies	Core Samples	Average Horizontal K (arithmetic)	Average Vertical K (arithmetic)	Average Porosity	Number of Core Photograph models
Sand	66	6622	5669	0.35	100
IHS	34	5479	5115	0.33	99
Breccia	31	7696	7123	0.36	99
Total	131	6405	5668	0.34	297

Modeling IHS

The layered nature of IHS results in thin sand beds that are the main conduit of flow at the scale considered. The geometric orientation of these layers can affect upscaled k_v and k_h . Literature suggests that the typical dip of IHS sets in the McMurray formation can range from 8°-15° degrees with minimums and maximums observed between 3°-30° (Mossop and Flach, 1983; Smith, 1987; Crerar 2007); however, the distribution of dips as measured by the automatic variogram fitting is much smaller because the apparent dip, not the true dip, is measured. As the true dip increases, k_h decreases and k_v increases. It is important to fully understand what effect a larger true dip has on the permeability relationships inferred. In this section, numerical experiments are conducted to assess the sensitivity of flow properties to the unknown true dip. It should be noted that in the presence of FMI data this is less of a concern as FMI provides 360° coverage of the borehole wall that can be used to infer the true dip of the IHS set (Strobl et al. 2009).

The impact of dip on the ϕ - k_h - k_v relationships is assessed by assuming a range of true dips. First, consider the apparent dip to be the true dip. The variogram from the 2D core photograph is fit automatically and the dip determined (Figure 5 right). This variogram is used with SIS to generate sand/shale models and results in the relationships shown in Figure 6. Of interest to modeling is the actual ϕ - k_v and ϕ - k_h relationships and how they are affected when the true dip is not measured.

The true dip is assumed to be 5°, 10°, 15° and 20° and the relationships (Figure 6) are recalculated. A corrected variogram (Figure 5 right) is calculated by determining the strike relative to the core photograph orientation (Equation 2) where the apparent and true dips are known. The corrected variogram is used in SIS and the methodology repeated for each core photograph. Rather than repeat all plots (Figure 6) for each true dip considered, the relationships are fit and compared (Figure 7). For high porosity values, the difference when considering the true dip is small. However for porosity values that are common in the McMurray formation there are significant differences in the modeled horizontal and vertical permeability values when considering the true dip. Higher porosity models are less affected

because there is less connectivity of the small proportions of shale and the orientations of these disconnected features are not as relevant to the flow response of the model.

$$\sin(\text{strike}) = \frac{\tan(\text{apparent dip})}{\tan(\text{true dip})} \quad (2)$$

If FMI data is available, an attempt should be made at inferring the distribution of true dips in the layer considered and the variogram for each SIS realization altered to consider uncertainty in the true dip.

Modeling Breccia

SIS effectively models the linear spatial orientation of sand/shale in the IHS and sand facies. Typically breccia is observed to have large clasts with some variation in size (Figure 8). If SIS is used to model breccia, the resulting sand/shale realizations are not consistent with the known breccia geometry (Figure 8) resulting in an inaccurate flow response assessment.

Multiple point statistics are used to generate realizations that better honor breccia geometry. First a library of TIs that represent different geometries and shale proportions is generated. TIs are created using a randomized object based modeling algorithm. Objects are breccia clasts that are randomly seeded throughout the micro-model. The geometry of the clasts is randomly grown until the model has the correct fraction of shale. Clasts are grown according to anisotropy and volume statistics that are derived from core photographs of breccia facies so that the models reflect the observed geometry. Generated clasts can be convex and nearly elliptic shaped to highly non-linear non-convex shaped by allowing growth to occur from the original seed point or by allowing the seed point to move using a random walk process.

Consider the 2D indicator model shown in Figure 8. To select the most appropriate TI for this set of conditioning data, the distribution of runs (Mood, 1940) for the conditioning data is compared to the distribution of runs of each TI in the library with similar proportions. The TI most similar to the conditioning data in a minimum squared error sense, is used in SNESIM (Strebelle 2000) to generate the categorical models for Breccia (Boisvert, Pyrcz and Deutsch, 2007).

Results

The bivariate relationships provided by micro-modeling are largely consistent with the core samples available (Figure 9). In general, the horizontal continuity due to the layered shale significantly reduces vertical permeability as indicated by the micro-modeling results. A new contribution to the micro-modeling workflow made in this work is accounting for the lack of orientation data from the core photographs. This source of uncertainty is quantified by assuming the dip observed in the photographs of IHS facies is an apparent dip. Introducing variability in the true dip of the micro-models provides a more complete understanding of the variability in ϕ , k_h , and k_v . The effects can be significant. Consider Figure 7: the vertical permeability for a porosity of 20% is roughly an order of magnitude higher for a true dip of 20 degrees than for the apparent dip. This would lead to large differences in flow performance prediction.

The focus of this work is establishing the micro-model scale ϕ - k_h and ϕ - k_v relationships. Normally, these relationships are then used in mini-modeling to obtain the porosity-permeability relationships at the scale of geomodeling or flow simulation. Mini-modeling is not considered in this work due to space constraints. It is recommended that unconditional realizations of porosity at the geomodeling scale of interest (usually $\sim 1\text{m} \times 1\text{m} \times 1\text{m}$ with $\sim 10\text{cm}$ blocks) be generated. Using a cloud transformation and the micro-modeling relationships developed, 3D realizations of permeability can be generated and upscaled. This provides the ϕ - k_h - k_v relationship at a geomodeling scale. Deutsch (2010) provides additional details on mini-modeling.

Conclusions

Integrating the micro-modeling methodology into a typical reservoir characterization workflow takes advantage of the large number of core photographs available. Beyond core photographs and FMI data there is little information available for the ϕ - k_h - k_v inference; biased core samples cannot be relied upon to obtain a reasonable understanding of the geocellular modeling scale relationship for all porosity ranges. The small scale spatial arrangement of sand and shale dominates the overall behavior of each facies and can be incorporated in micro-modeling. The techniques presented generate and assess the

reasonableness of micro-models for better inference of porosity-permeability relationships, which is a critical and data-poor aspect of any reservoir modeling work flow.

References

- Boisvert, J.B., Pyrcz, M.J., Deutsch, C.V.: Multiplepoint statistics for training image selection: *Nat. Resour. Res.*, 16(4),313–321 (2007)
- Crerar E., Arnott R.: Facies distribution and stratigraphic architecture of the Lower Cretaceous McMurray Formation, Lewis Property, northeastern Alberta. *Bulletin of Canadian Petroleum Geology*, v. 55. no. 2 99-124 (2007)
- Deutsch, C.V.: A probabilistic approach to estimate effective absolute permeability. PhD Thesis, Stanford University, Stanford, CA. 165 pages. (1987)
- Deutsch, C.V.: *Geostatistical Reservoir Modeling*. Oxford University Press Inc., New York, N.Y. (2002)
- Deutsch, C.V.: Estimation of vertical permeability in the McMurray Formation. *Journal of Canadian Petroleum Technology*. (12), 1-9 (2010)
- Government of Alberta: Alberta Energy: Facts and Statistics. Available via: <http://www.energy.alberta.ca/OilSands/791.asp> Cited 20 Feb 2011.
- Kolbjornsen, O. and Abrahamson, P.: Theory of the cloud transform for applications. In: *Proceedings of the Seventh International Geostatistics Congress, Banff, Alberta*, 45-54. (2004)
- Mood, A. M.: The distribution theory of runs: *Annal. Math. Stat.*, 11(4), 367–392 (1940)
- Mossop, G.D., Flach P.D.: Deep channel sedimentation in the Lower Cretaceous McMurray Formation, Athabasca Oil Sands, Alberta. *Sedimentology*, 30(4), 493-509. (1983)
- Olson, J.E., Yaich, E., Holder, J.: Permeability changes due to shear dilatancy in uncemented sands. In: *Proceedings of the 43rd US Rock Mechanics Symposium, Asheville, NC*. (2009)
- Shang, R. and Wang, W.H.: Sedimentary Texture Characterization and Permeability Anisotropy Quantification of McMurray Oil Sands. Abstract in: *Gussow Geoscience Conference, Banff, Alberta*. (2011)
- Smith, D.G.: Meandering river point bar lithofacies models: modern and ancient examples compared. In: *Ethridge, F.G., Flores, R.M. and Harvey, M.D. (eds), Recent developments in fluvial sedimentology*. Society of Economic Paleontologists and Mineralogists, Special Publication Number 39, 83-91. (1987)
- Strebelle, S.: Sequential simulation drawing structures from training images. PhD Thesis, Stanford University, Stanford, CA. 187 pages. (2000)
- Strobl, R., Ray, S., Shang, R., Shields, D.: The Value of Dipmeters and Borehole Images in Oil Sands Deposits - A Canadian Study. *CSPG CSEG CWLS convention*. 7 (2009)
- Thomas, R.G., Smith, D.G., Wood, J.M., Visser, J., Calgerley-Range, E.A., Koster, E.H.: Inclined Heterolithic Stratification-Terminology, Description, Interpretation and Significance. *Sedimentary Geology*. (53)1-2, 123-179 (1987)
- Tran, T.T.: The missing scale and direct simulation of block effective properties. *Journal of Hydrology*, 182, 37-56 (1996)

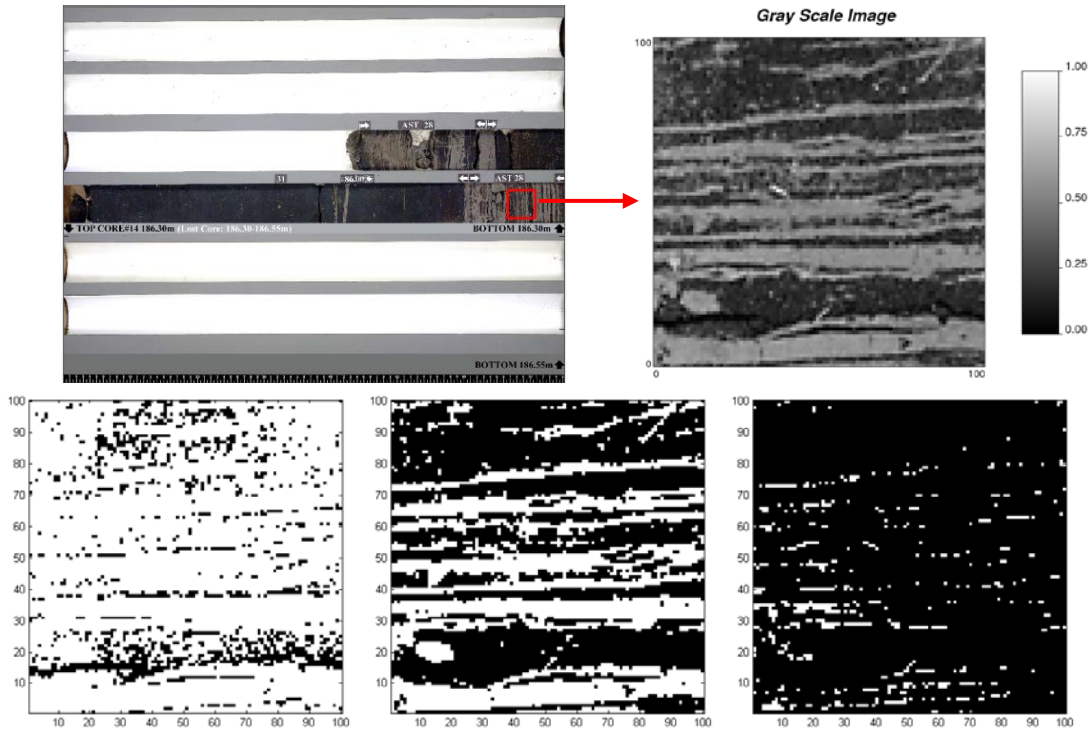


Figure 1: Above: Gray scale image and indicator variogram using the appropriate cutoff. Below Left: Cutoff selected is too low. Below Right: Cutoff selected is too high. Below Center: Appropriate cutoff value.

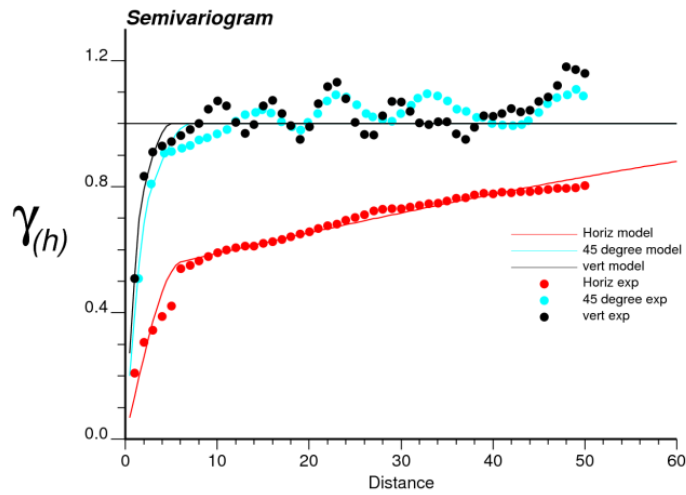


Figure 2: Vertical (black), horizontal (red) and 45° dip (blue) modeled variograms for the data in Figure 1.

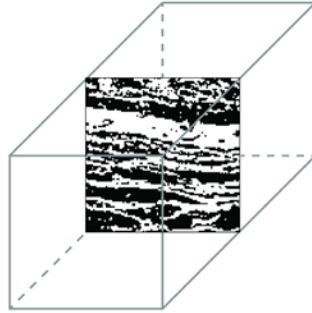
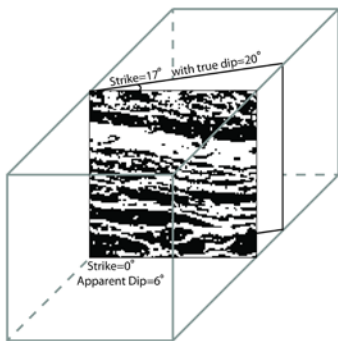


Figure 3: Sand (black) and shale (white) conditioning data from a core photograph for one micro-model.



Figure 4: Core photograph exemplars for the facies modeled. Above: Sand. Middle: IHS. Below: Breccia.



apparent dip=6° strike = 0°

$$\gamma(h) = 0.68sph_{a6^\circ=5.5} + 0.32sph_{a6^\circ=373}$$

$a_{96^\circ}=2.0$ $a_{96^\circ}=5.9$

true dip=20° strike = 17°

$$\gamma(h) = 0.68sph_{a20^\circ=5.5} + 0.32sph_{a20^\circ=373}$$

$a_{110^\circ}=2.0$ $a_{110^\circ}=5.9$

Figure 5: Left: Conditioning data showing strike of 17° assuming a true dip of 20°. Right: automatic variogram fitting dip=6°. Variogram is isotropic in both horizontal directions.

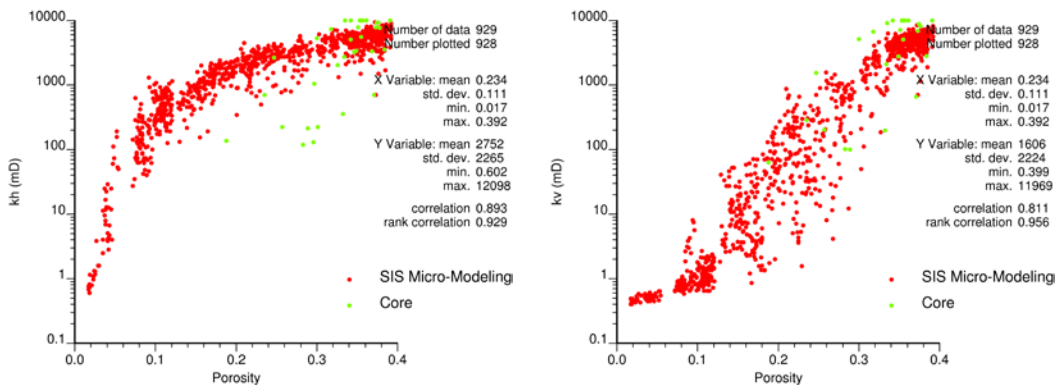


Figure 6: Relationships of interest for IHS using the apparent dip.

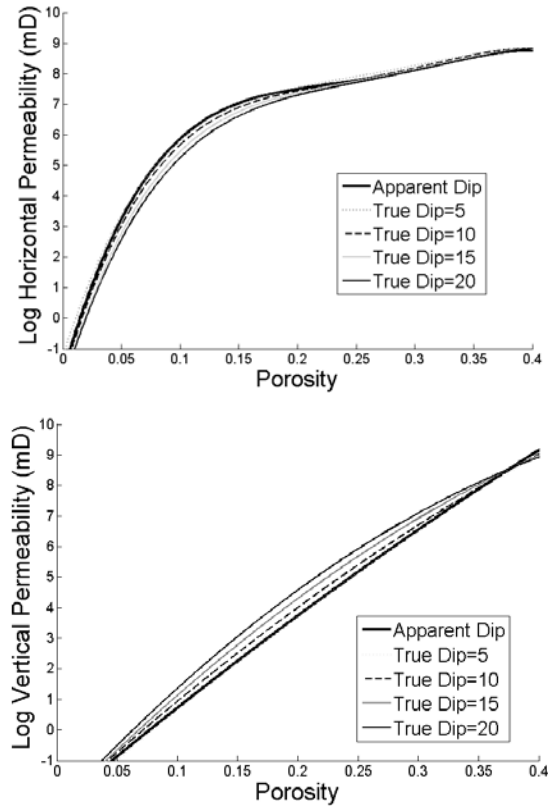


Figure 7: ϕ - k_h and ϕ - k_v relationships for different true dip in IHS facies.

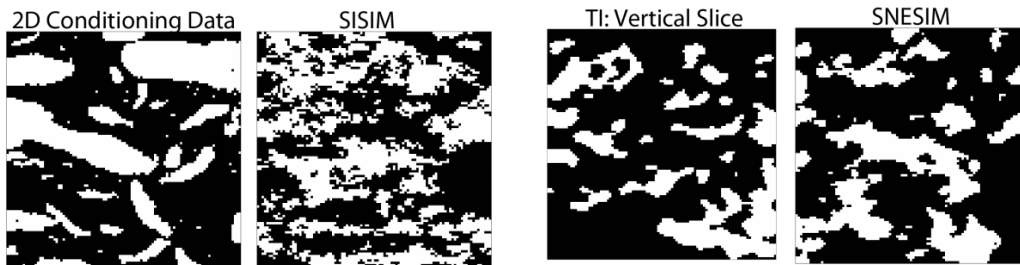


Figure 8: From Left: 2D Breccia model from the core photograph. One slice of an SIS realization of breccia. Slice from the TI used in SNESIM. SNESIM realization slice.

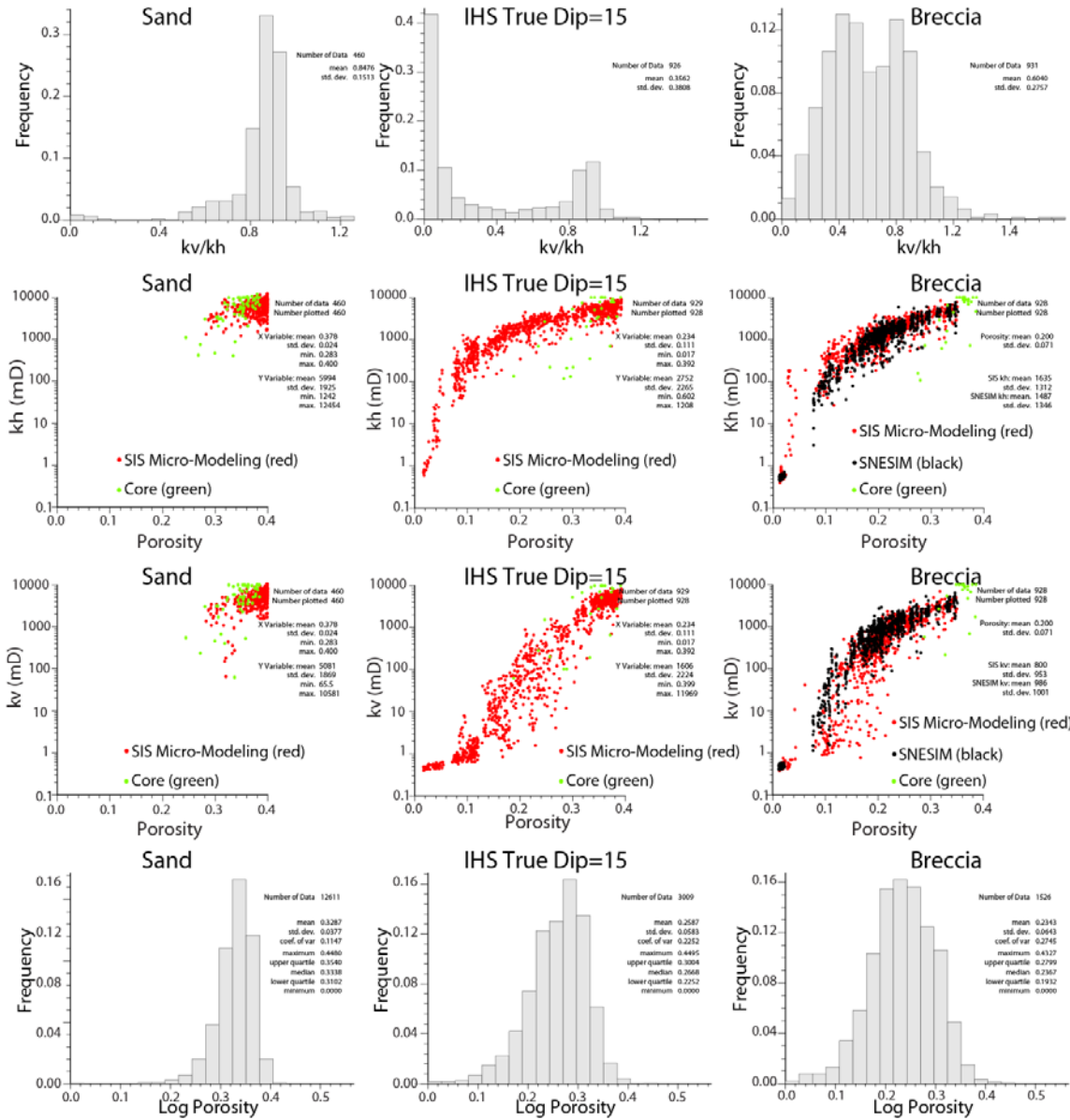


Figure 9: Summary relationships.